Finite element microstructural homogenization techniques and intergranular, intragranular microstructural effects on effective diffusion coefficient of heterogeneous polycrystalline composite media.

***S. Jothi, T. N. Croft, S. G. R. Brown, E. de Souza Neto**
College of Engineering, Swansea University, Singleton Park, Swansea SA2 8PP, UK
*S.Jothi@swansea.ac.uk

ABSTRACT

Microstructural intergranular and intragranular effects play a vitally important role in mass transport within heterogeneous polycrystalline composite media. Full scale macroscopic specimen or component modelling of heterogeneous polycrystalline composite media is complex, time consuming and computationally expensive. Consequently it is important to develop a homogenous model to predict the effective diffusion coefficient of the heterogeneous polycrystalline composite media. It is also important to investigate the effect of intergranular and intragranular microstructure on effective diffusivity of heterogeneous polycrystalline composite media. A two dimensional finite element microstructural representative volume element (FEMRVE) model with different intergranular and intragranular microstructures has been developed using the well-known Voronoi tessellation technique. The effective diffusivity predicted by the FEMRVE model with various intergranular and intragranular microstructures of heterogeneous polycrystalline composite media agrees well with the results of various effective medium theories.

Keywords: Diffusion; Polycrystalline composite; Microstructure; Intergranular; intragranular; homogenization

1. Introduction

Even though there is a considerable amount of information about the embrittlement mechanism of polycrystalline structural materials [1-6], there are still number of different types of pending embrittlement problems caused by atomic mass transport of impurity elements (hydrogen, sulphur, oxygen, carbon, nitrogen, boron etc.) and inclusion elements that are not clearly understood [7,8,11,20-23,25,26,28]. By better understanding microstructural intergranular behaviour of high performance polycrystalline materials, the embrittlement problem may be solved by expanding the concept of microstructural intergranular engineering into design and analysis [8, 24]. One such example of

understanding microstructural intergranular behaviour of polycrystalline material produced an innovative solution for repairing the nuclear steam generator using electrodeposition of continuously bonded nanocrystalline nickel [27]. Mass transport properties of impurity elements such as hydrogen and sulphur in the polycrystalline material are one of the pending embrittlement problems [4, 6, 9-12].

Prediction of the effective mass diffusion property of advanced heterogeneous microstructural polycrystalline composite material has been an active research area for many years [14, 17-19, 29]. Fisher [14] developed an analytical model for two phase heterogeneous crystalline composite material by considering the fast diffusion along the single isolated grain boundary embedded with slow diffusion in the bulk which is overgeneralized for polycrystalline material. Hart [17] developed an analytical model to predict the effective diffusivity of two phase dislocation and intragranular heterogeneous microstructural composite material based on composite rule of mixture method. Hart's model was modified by Mortlock [29] and Kalnin [30] by taking into account of segregation for parallel and series intergranular phase. Later the analytical model was demonstrated to be valid for a realistic two phase heterogeneous polycrystalline material [38, 31]. Wang *et al*. [18] developed a model based on the same composite rule of mixture for three phase heterogeneous polycrystalline microstructural composite material by including the triple junction as the third phase. In the past few decades, a number of analytical micromechanical studies have been reported in the literature [14, 17-19] to predict the effective mass transport property by treating heterogeneous materials containing intergranular and intragranular microstructures as a composite media. A robust polycrystal mass diffusion numerical model is essential for forecasting the effective mass transport property of realistic heterogeneous polycrystalline materials [13]. The diffusion behaviours of the polycrystalline materials are strongly affected by the microstructural phases [1-4, 6, 9-12]. Intergranular and intragranular distribution plays a key role in determining their diffusion behaviour. The intergranular phase consists of grain boundaries and triple junctions and the intragranular phase contains the grains and the defects throughout this model.

It is anticipated that the diffusivity in intergranular phase has a higher value than the intragranular phase in this work as reported by many researchers. A few examples of this trend are; Tsuru *et al*. [4] investigated the diffusion permeability of hydrogen along intergranular and intragranular phase in heterogeneous polycrystalline pure nickel (99.97 % Ni) Ni 270 material with average grain size of about 100 μm and an implicit grain boundary

thickness of 1 μm and observed the hydrogen diffusion coefficient along the intergranular phase was approximately 60 to 100 times accelerated compared to the intragranular phase. Harris and Latanision [2] studied the hydrogen diffusivity along grain boundary in fine grained nickel produced by electrodeposition and estimated the hydrogen diffusion coefficient along the grain boundary is 40 times larger than lattice diffusion at 30 °C. Palumbo *et al.* [1] determined that the hydrogen diffusion in the grain boundary is approximately 70 times faster than within the intragranular region in electrodeposited nano polycrystalline Ni with average grain size of 17 nm. Some other researchers demonstrated faster diffusivity in intergranular phase than intragranular phase in Face Centred Cubic(FCC) structural materials, examples of this can be found in Bokstein *et al.* [5], Oudriss *et al.* [3]. Portavoce *et al.* [6] determined higher diffusion of mass atom in intergranular phase than in intragranular phase in heterogeneous polycrystalline silicon material. Hoffman and Turnbull [15, 16] observed the self-diffusion of silver in a grain boundary was several orders of magnitude greater than in the lattice.

The Voronoi tessellation technique is a well-established approximation technique used to model the actual microstructure of polycrystalline materials (see e.g. Ghosh *et al.* [13]), in order to avoid the problems inherent in experimental techniques [33-37] as stated in Table 1. The objective of this study is to develop a numerical finite element microstructural homogenization technique and microstructural finite element model with intragranular and intergranular phase constituent, to calculate the effective mass transport coefficient and to investigate the microstructural effects on the heterogeneous polycrystalline composite media. Initially the Voronoi tessellation technique is adopted to geometrically represent the heterogeneous polycrystalline material to allow the exploration of the effect of average grain size and intergranular phase thickness.

Table1: Experimental technique to measure the real microstructural topography of polycrystalline materials and its difficulties.

S.No	Experimental techniques	Measurements	Difficulties
1	X-ray Computer micro tomography	Microstructures such as grains and micro cracks	In determining the orientation of intragranular microstructural phases such as grains [33]
2	Electron back scatter diffraction methods	Microstructure including orientation of intragranular phase constituent such as grains	Expensive, complicated, Impossible to gain data from large number of samples and in order to get significantly high spatial resolution the sample size should be very small i.e. there will be compromise between maximum sample size and resolution [34, 35].
3	Ion beam serial	Microstructural	Post processing is complicated and requires

	sectioning electron back scatter diffraction method	morphology	enormous aggregate data which leads to non-unique topologies owing to the overlapping of intragranular phase constituent [35, 36, and 37].

Secondly, the geometric model was combined with the finite element method in the form of 2D representative volume element (RVE) model. This was implemented in the finite element commercial software ABAQUS to allow the prediction of the effective hydrogen diffusion of composite constitute Intergranular and intragranular polycrystalline material. Next, simulation results of these models were verified by analytical effective medium approximation theory results. Finally in this contribution, the effects of grain size and its relationship with intergranular microstructural phase character, distribution and the effective mass diffusion in the heterogeneous polycrystalline aggregates composite media are discussed.

2. Simulation methods and applied polycrystalline microstructure, finite element model

2.1 Heterogeneous polycrystalline microstructure model

The mechanisms of a computationally modelled heterogeneous polycrystalline microstructure and the effects of average intragranular phase size and intergranular phase are presented here. Voronoi tessellation techniques were adopted to geometrically model the polycrystalline material. The 2D polycrystalline microstructure was randomly created as polygonal intragranular phase grains surrounded by zero intergranular phase thickness in the fixed 2D plane area. The grains were generated by calling the Voronoi generation function in MATLAB. Seeds for the Voronoi polygon grains were generated using random points. Then by averaging the vertices of each cell the centre point of these random polygons grain cells were calculated. Interior Voronoi polygon grains are generated using the calculated centre points and by matrix arithmetic, as shown in (1), the random intergranular phase thickness was introduced into the polycrystalline microstructure as shown in the Figure 1. Each polygon intragranular phase is surrounded by the intergranular phase thicknesses which are shared by the adjusting polygon grains to form random polycrystalline microstructure with random intergranular phase as shown in the Figure 2. The average thickness of the random intergranular phase are controlled by the controlling the number of seeds. The average size of the intragranular polygon phase grains and its distribution are controlled by controlling the number of seeds and its relative position in the fixed representative area element.

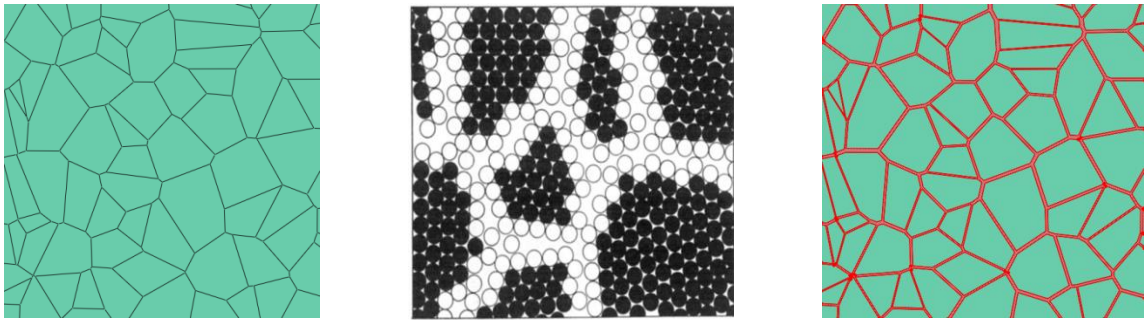

(a) **(b)** **(c)**

Figure 1: Polycrystalline microstructures (a) With zero intergranular phase thickness (b) Atomic structure of a two dimensional model of nanostructured material. The atoms in the centres of the crystals are indicated in black represented as grains. The one in the boundary core regions are respected as open circles represented as grain boundaries [32] (c) With nonzero random intergranular phase thickness.

$$(ipvx, ipvy) = (1 - \delta) * (opvx, opvy) + \delta * (cmx, cmy) \quad (1)$$

The (1) $ipvx, opvx$ are the inner and original centre polygon vertices x-coordinate values respectively, $ipvy, opvy$ are the inner and original centre polygon vertices y-coordinate value respectively, cmx, cmy are the calculated centre point of original centre closed polygon coordinates of x and y coordinate values respectively and δ is the average thickness of the random polygon.

MATLAB code was developed, to determine the inner Voronoi polygon grain cells edges, vertices, and centre for each randomly generated polygon of the polycrystalline microstructures and these data were exported to the PYTHON programming language. Then PYTHON code was developed to import the inner and outer Voronoi polygon grain cells data and by using these data, lines were drawn for each polygon cells vertices and to partition the faces of each polygon. An average random intergranular phase thickness, an example with 5 nm used for an approximate average grain size of 100 μm is shown in Figure 2, was generated in MATLAB. The heterogeneous polycrystalline microstructures for different approximate average intragranular polygon grain size of the range from 100 μm to 0.01 μm by incrementally downscaling the grain size by one order were simulated. According to many researcher results, the importance of triple junctions is significant when the average grain sizes are less than 10 nm [7], so in this paper the triple junction is not specify as separate phase rather its incorporated with the intergranular phase.

The developed MATLAB, PYTHON code were compiled to harvest the different average intragranular polygon phase grain size, different surface area per unit volume intergranular microstructure, different average intergranular phase thickness and different volume fraction of intergranular microstructure by changing the number of Voronoi seeds/ scale factors, thickness between the interior and exterior Voronoi diagrams.

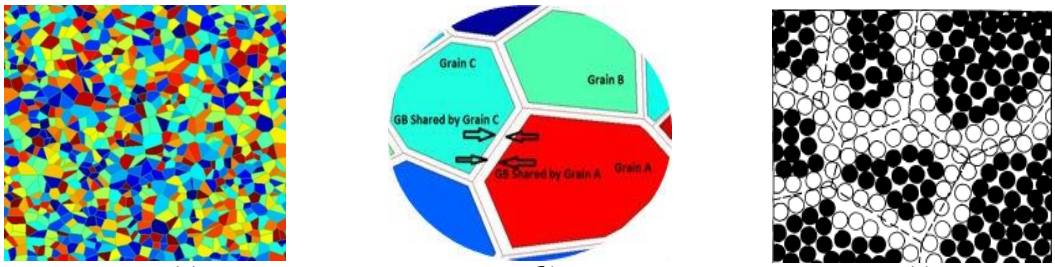

(a) **(b)** **(c)**

Figure 2: (a) Computationally generated 2D Representative volume element of heterogeneous polycrystalline microstructures with average random intergranular phase thickness of 5 nm and approximate average intragranular polygon phase grain size of 100 μm. (b) Heterogeneous Polycrystalline microstructures with random intergranular phase shared between adjusting polygon intragranular phase. (c) Schematic cross section through a two dimensional nanoglass. The atoms are represented by circles. The material consists of small regions in the interior of which (filled circles) the interatomic spacing are similar to a bulk glass. In the interfacial region (broken lines, open circles) a broad spectrum of interatomic spacings exists [42].

2.2 Finite Element heterogeneous polycrystalline microstructure composite model

The commercial finite element software ABAQUS was employed to develop the finite element heterogeneous polycrystalline microstructure composite model. The developed PYTHON script was compiled in ABAQUS to generate the random heterogeneous polycrystalline phase mixed intergranular and intragranular microstructure. A mesh convergence study was then performed in ABAQUS to eliminate the mesh sensitivity and to ensure the precision of the analysis. The number of elements used was based on the mesh convergent study. Triangle elements were generated and used due to the complexity of the geometry of the model. Then the intergranular and intragranular phases were given different diffusion properties according to the constitutive equations. The diffusivity parameter of intragranular phase and intergranular phase used in this finite element model were of the order of 9×10^{-14} m^2/s and 4×10^{-10} m^2/s respectively.

3. Finite element microstructural homogenization technique and procedure

In the homogenization technique, it is the practice of most of the micromechanical models to consider the RVE of heterogeneous microstructural distribution in the periodic

arrangement to reduce the complexity of the analysis and for computational efficiency. Figure 3 shows the heterogeneous macroscopic polycrystalline composite media and the intergranular and intragranular microstructural RVE. In a heterogeneous composite polycrystalline media, the actual microstructural intergranular and intragranular distributions are random. The 2D random intergranular polygon and random intragranular microstructural distribution generated as explained in the previous section were taken as microstructural representative volume element (MRVE) and implement in the finite element model to generate the 2D finite element microstructural representative volume element model (FEMRVE).

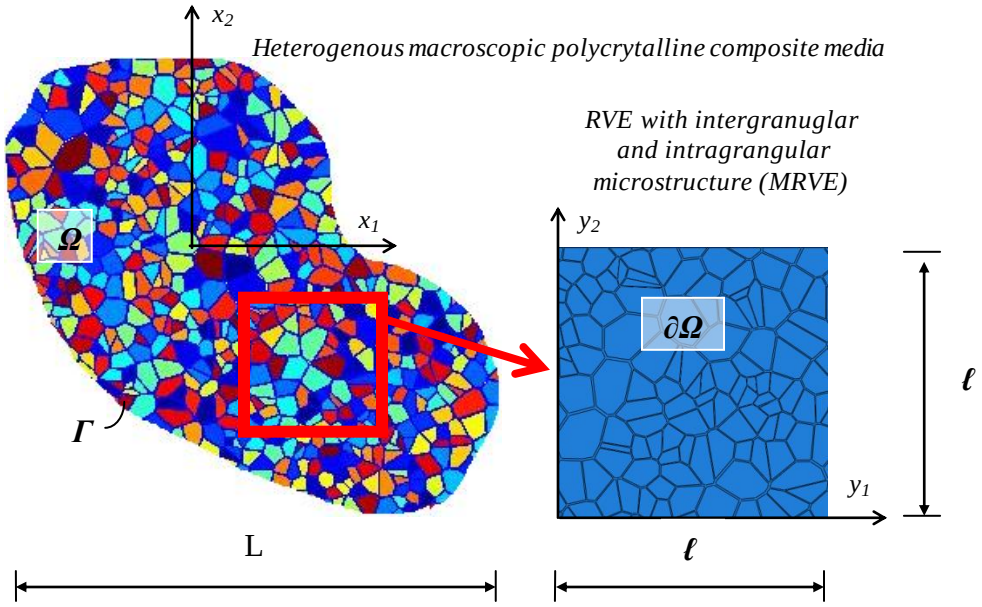

Figure 3: Heterogeneous polycrystalline composite media and microstructural representative volume element.

This MRVE has the same mass transport properties and intragranular volume fraction as the composite media. The heterogeneous MRVE were embedded with the homogeneous RVE (HRVE) to global RVE (GRVE) as shown in the Figure 4(a) to make it easier to find the unknown effective composite mass transport constant. Both the heterogeneous MRVE and HRVE have the same mass transport constants. Normally, the heterogeneous polycrystalline composite media is modelled as a homogenous media with certain effective mass transport properties that describe the average mass transport properties of the heterogeneous polycrystalline composite media.

In the present work, the mass transport equations are solved numerically. The governing equations for a macroscopic two dimension domain, that is, $\boldsymbol{\Omega}$, made of heterogeneous

polycrystalline composite media. The microstructural response of material were analysed using RVE of microscopic length scale ***(ℓ)***, where microscopic size scale is much small than the macroscopic length scale (***L)***. The length scales ratio is represent by small parameter ***ε=ℓ/L*** where **ε** is small parameter ***0 < ε << 1***. Thus, with microscopic two dimension domain ***∂Ω*** is the so called FEMRVE and small parameter ***ε>0,*** the material functions just introduced are ***ε.∂Ω*** periodic in local variable ***y=x/ε*** and for each ***x*** ϵ ***Ω***. All the field variables are assumed to depend on macroscopic **(*x*),** microscopic **(*y*)** and time **(*t*)** as ***Φ(x,y,t) = Φ(x,x/ε,t)***.

3.1 Macroscopic problem

The steady state mass flow equilibrium of macroscopic ***Ω*** domain**,** are as shown in the below equation.

$$\frac{\partial J_i}{\partial x_j} = 0 \qquad \text{in } \boldsymbol{\Omega} \tag{2}$$

Where the $\partial J_i / \partial x_i$ denotes the rate transfer of mass flux vector through the macroscopic unit area, the suffix ***i*** denotes the directions. Mass production and transient mass transport are excluded in this work.

$$J_i n_i = \tilde{J} \quad \text{on } \Gamma \tag{3}$$

Where $\tilde{J}$ is the mass flux prescribed normal to the boundary Γ, n_i is the vector component outward normal to the boundary. The virtual mass concentration field ***C*** with sufficient regularity must vanish on the part of boundary ***Γ*** where mass concentration is prescribed.

The constitutive equation for the mass flux at any point in macroscopic Ω domain is given by

$$J_i(\boldsymbol{x}) = -\boldsymbol{D}_{ij}(\boldsymbol{x}).\left(\frac{\partial C}{\partial x_1} + \frac{\partial C}{\partial x_2}\right) \tag{4}$$

$$J_i(\boldsymbol{x}) = -\boldsymbol{D}_{ij}(\boldsymbol{x}).\nabla C_j(\boldsymbol{x}) \tag{5}$$

Where $\boldsymbol{D}_{ij}$ stands for the second order diffusivity of mass transport second order tensor.

The local properties are assumed to be isotropic in this work. The considered volume of the heterogeneous material the field $\boldsymbol{D}_{ij}$ is known according to the underlying intergranular and intragranular microstructure.

According to the uniform mass flux at the boundary, the mass flux at any point $\boldsymbol{x} \boldsymbol{\epsilon} \boldsymbol{\Gamma}$ is given by the below equation. To describe the macroscopic homogeneous media, the steady state micro mass flows through the microscopic domain were volume averaged as shown in the below equation.

$$\overline{J_i(x)}.n_i = J_i(y).n_i \tag{6}$$

$$\Rightarrow \quad \overline{J_i(x)}(x) = \langle J_i(y) \rangle \tag{7}$$

$$\overline{J_i(x)} = \langle -\boldsymbol{D_{ij}}(\boldsymbol{y}).\nabla C_i(\boldsymbol{y}) \rangle \tag{8}$$

Where $\overline{J_i(x)}$ is the macroscopic mass flux and $J_i(y)$ is the microscopic mass flux.

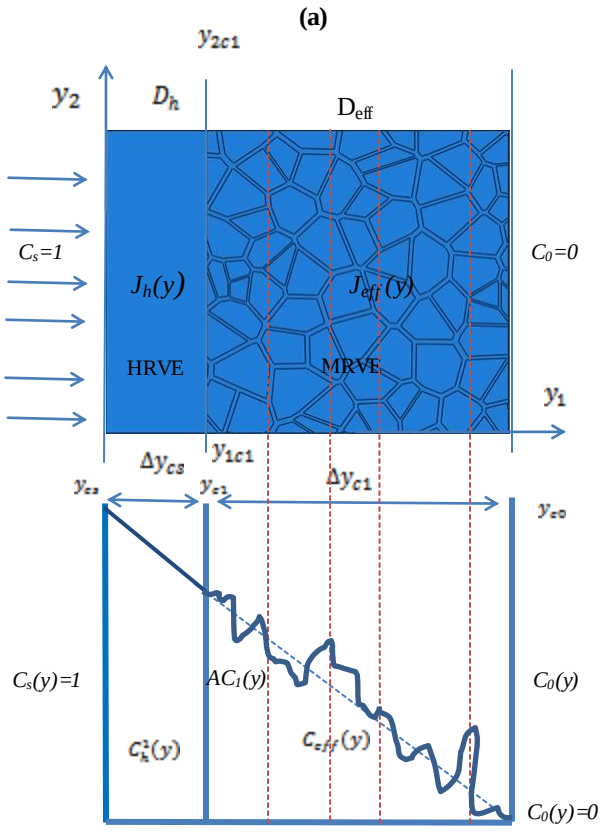

Figure 4: (a) GRVE with MRVE embedded with HRVE1 (b) Mass concentration profile in HRVE and with increase or decrease at MRVE due to intergranular microstructures.

3.2 Microscopic problem

The two dimensional heterogeneous polycrystalline microstructural composite media formed by periodically distributed polycrystalline intragranular and intergranular microscopic

regions with the diffusion coefficient D_{ig} and D_{gb}, respectively and its effective diffusion coefficient D_{eff} as shown in the Figure 4(a) is considered**.** The corresponding concentrations are denoted by $C_g(y)$, $C_{gb}(y)$ and $C_{eff}(y)$. According to the effective medium theory, the macroscopic heterogeneous polycrystalline composite periodic media were replaced by the MRVE consisting of randomly generated polygon grains as intragranular microstructure and randomly generated grain boundaries embedded between the polygon grains as intergranular microstructure, which are embedded into the homogenous RVE (HRVE) with the diffusion coefficient D_h and concentration $C_h(x)$ as shown in Figure 4(b). The Global RVE (GRVE) is the whole and consists of HRVE and hetero subdomains/substructure MRVE. The direction of the mass flow is from left to right through GRVE which was normal to the interface of the MRVE and HRVE.

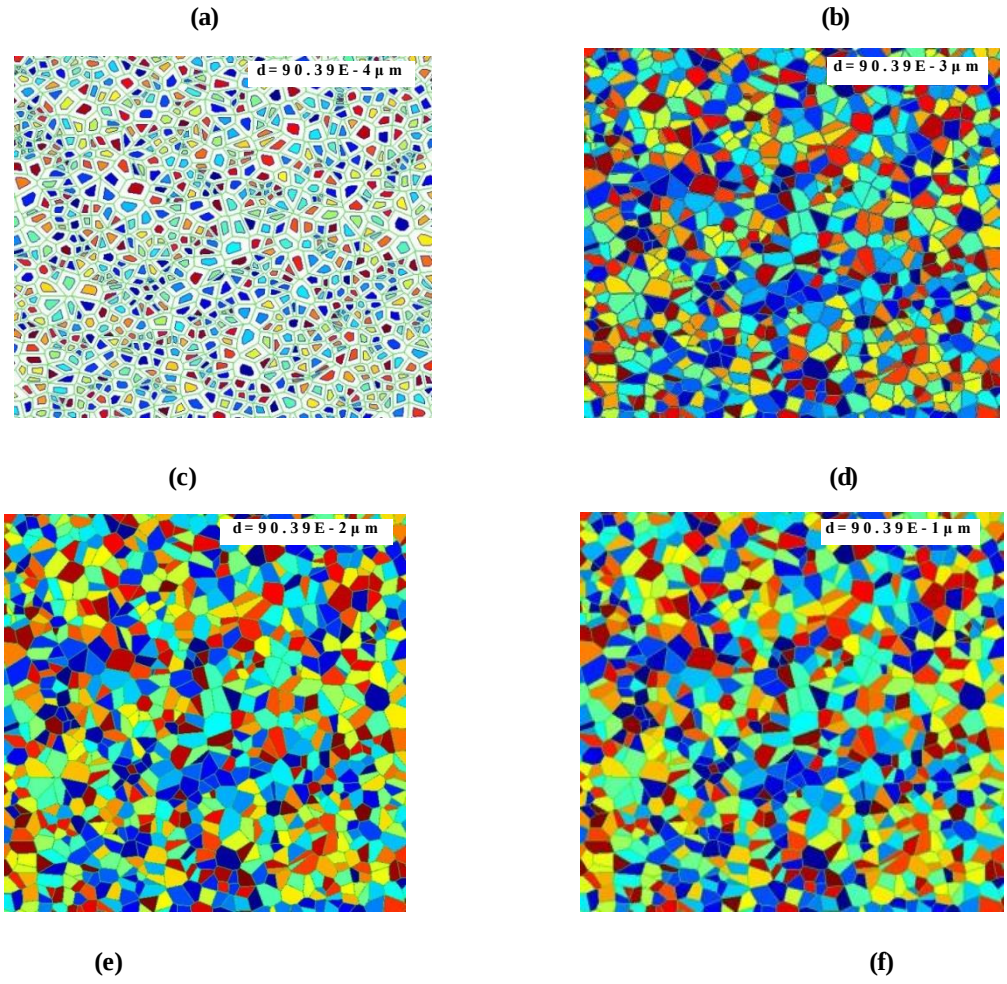

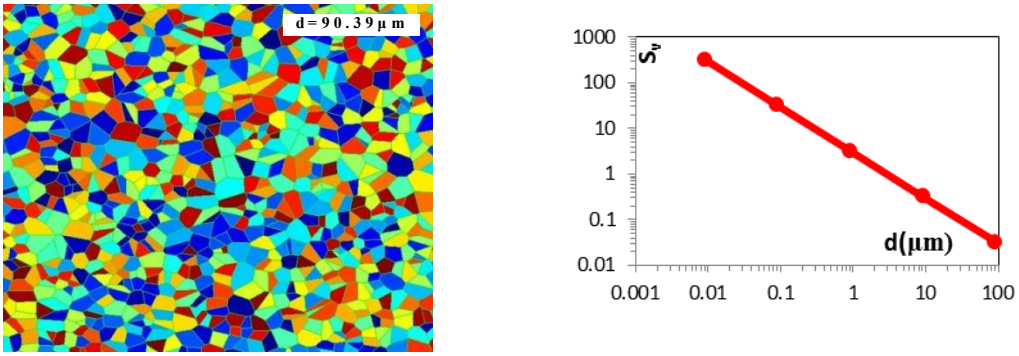

Figure 5: Computationally generated microstructure model (a-e), (f) Average surface area to the volume ratio of grains as the function of average grain size.

The HRVE diffusion constant was taken as any value in between the D_{ig} and D_{gb} microstructural diffusion constant. The driving mechanism for mass transport is the concentration gradient developing in the volume as the result of boundary conditions.

Under the steady state condition the mass flux in the MRVE is equal to the mass flux in HRVE, which makes the two RVE mass fluxes are equal as shown in the below equation. The boundary conditions are

$$\therefore \quad J_{h1}(y) = J_{eff}(y) \tag{9}$$

$$D_h \frac{\partial C_h^1}{\partial y_1^1} = D_{eff} \frac{\partial C_{eff}}{\partial y_1^2} \tag{10}$$

$$D_h^1 \frac{(AC_1 - C_s)}{(y_1^2 - y_1^1)} = D_{eff} \frac{(AC_0 - AC_1)}{(y_1^s - y_1^2)} \tag{11}$$

Where $AC_1 = \int_{y_{2c1}}^{y_{1c1}} C_1 \, dy_2$, $AC_0 = 0$ and $D_{eff}(D_{ig}, D_{gb}, k_{ig}, k_{gb})$

The effective mass diffusivity of the MRVE can be calculated using above equations.

$$D_{eff}(y) = k_{ig} D_{ig}(y) + k_{gb} D_{gb}(y) \tag{12}$$

In the above equation k_{ig} , k_{gb} are the intergranular and intragranular coefficients characterizing the effective mass diffusion of the MRVE respectively. The average mass diffusion coefficients obtained from the simulation results were compared with the effective medium approximation analytical results which is shown in result and discussion section 5.2 and section 5.2.

4. Effective Medium Approximation

The Maxwell-Garnett effective medium approximation [38, 39] and Hashin–Shtrikman upper bound effective medium approximation [40, 41] formula for heterogeneous polycrystalline composite media with intergranular and intragranular phases are as shown below respectively.

$$D_{eff} = D_{ig}\left[\frac{2D_{ig}V_{fig}+D_{gb}(1+2V_{fgb})}{D_{ig}(3-V_{fig})+D_{gb}(1-V_{fgb})}\right] \quad (13)$$

$$D_{eff} = D_{gb} + \left[\frac{V_{fig}}{\left(\frac{1}{D_{ig}-D_{gb}}\right)+\left(\frac{V_{fgb}}{3D_{gb}}\right)}\right] \quad (14)$$

Where, diffusivity of intragranular, intergranular phases and effective diffusivity are D_{ig} , D_{gb} and D_{eff} respectively. V_{fig} and V_{fgb} are volume fraction of intragranular and intergranular phase respectively.

The analytical models results of these effective medium approximations are compared with the numerical finite element calculation results in section 5.1 and section 5.2.

5. Results and discussions

Many researchers reported that the diffusion of mass in polycrystalline heterogeneous composite media could be affected by intragranular microstructure phase polygon grain size and intergranular phase which driven us to develop this model to study and investigate the mass diffusion properties as the function of microstructural effects. For the computation calculation five different composite polycrystalline media with average grain sizes of 90.39, 9.039, 0.9039, 0.09039, 0.009039 μm were modelled and its close view is shown in the Figure 5.

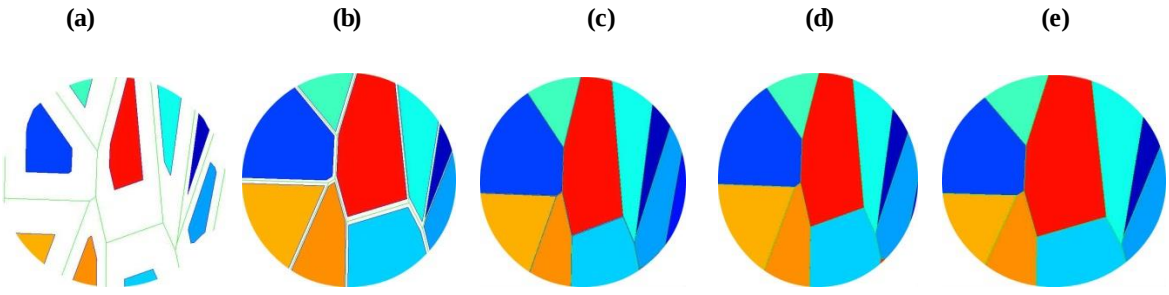

Figure 6. Close view of computed composite polycrystalline material with intergranular phase and its average grin size various from 9.039 nm, 90.39 nm, 903.9 nm, 9.039 μm, 90.39 μm respectively

The heterogeneous polycrystalline composite media microstructures are divided into intergranular phase and intragranular phase are distinguishable for the modelled average grain size 0.009039 μm since the intergranular phase occupies a significant portion of the heterogeneous polycrystalline composite as shown in the Figure 5(a).

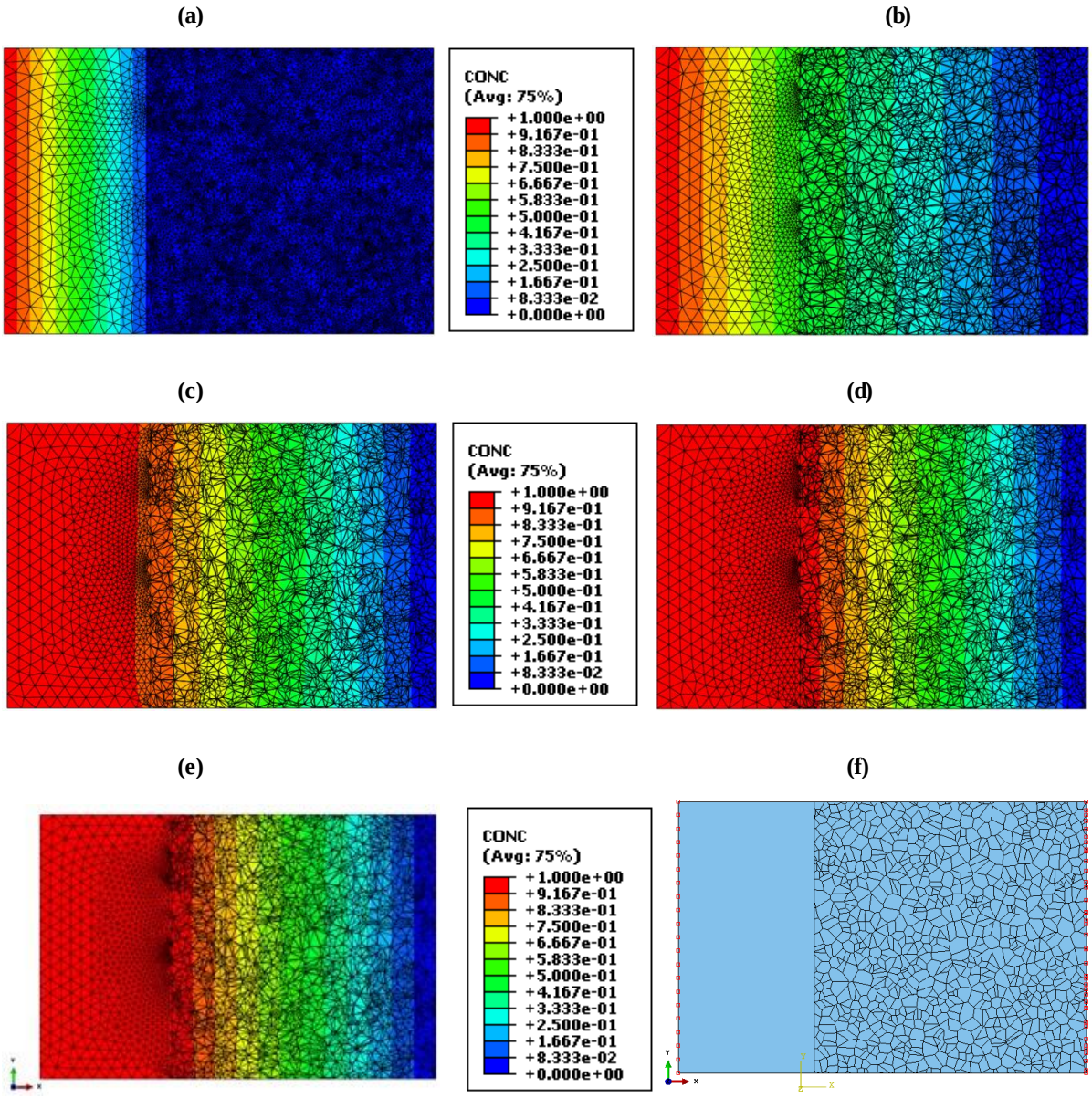

Fugure 7: (a-e) Cross section in the xy plane of the steady state mass concentration counter plot maps of global representative volume elements with microstructural representative volume element of five different average grain sizes starts from 0.009039 μm (9.039 nm) in the increased by one order to 90.39 μm. (f) Global representative volume element includes homogeneous representative volume element embedded with the microstructural representative volume element.

And for the remaining microstructures that were modelled, the grain sizes are barely distinguishable so the zoomed in close view of microstructures are shown in Figure 6 to

notice the difference between the intergranular and intragranular phase. The different mass diffusion response of the intergranular phase and intragranular phase are also incorporated. At the present stage, no attempt was made to consider the anisotropic effects for the mass diffusion. Mass diffusion coefficients for intergranular and intragranular microstructure are different. The diffusion of hydrogen concentrations for five different grain sizes from 90.39 to 0.009039 μm were coded using FE software and the calculations were carried out successfully.

Figure 7 shows the computed effective concentration of mass hydrogen for the different grain sizes (90.39, 9.039, 0.9039, 0.09039, 0.009039 μm). The grain size has significant effect on the effective diffusion of hydrogen in heterogeneous polycrystalline intergranular and intragranular microstructural composite structural materials.

5.1 Grain size relationship with intergranular phase character and distribution

In Figure 8(a) we plotted the average surface area of intergranular phase as a function of average grain size and the trend of the line found to be based on power law equation as shown in the below equation (15). The average surface area of intergranular phase increases when the grain size decreases.

$$S_{Aig}=k.d^{-n} \tag{15}$$

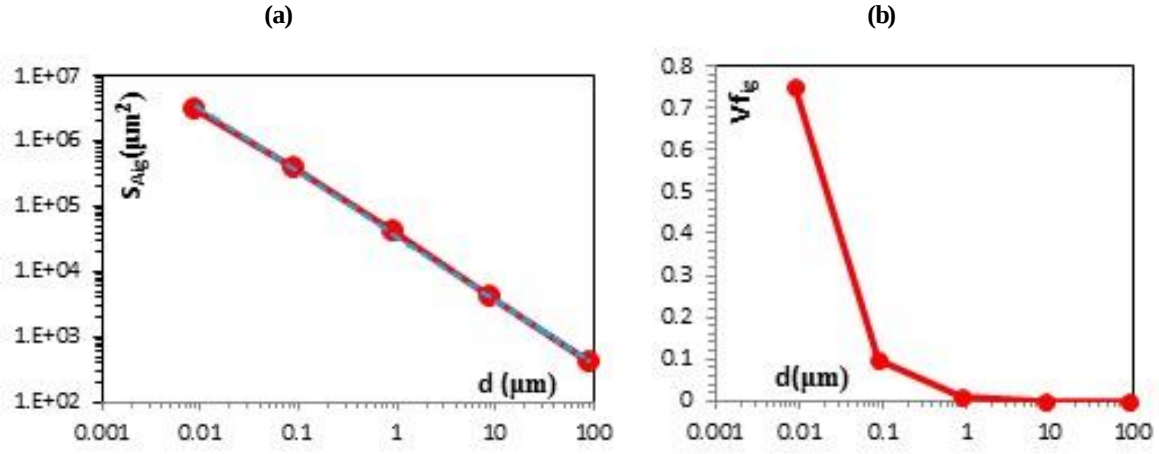

Figure 8: (a) Computational results of volume fraction of intergranular phase as a function of average grain size. (b) Computational results (solid line) and power law $A_{ig} \alpha d^{-0.972}$ (dotted line) of average surface area of intergranular phase (A_{ig}) as a function of average grain size.

The testing of intergranular microstructures characterized by different grain sizes shows the computational results of average surface area of intergranular phase are found to be dependent on the grain size. This confirms the ability of the model to predict the constants of

the power law equations which are in agreement with the trend expected according to the power law. This shows the clear relationship between the intergranular microstructure phase and the effect of grain size in heterogeneous polycrystalline materials, where the intergranular phase is not negotiable and has an important role.

Figure 8(b) shows the change in volume fraction of intergranular phase as the function of average grain sizes. The volume fraction of intergranular microstructure phase increases as the average grain size decreases. In the following discussion the results are divided into three ranges corresponding to differing average grains. The average grains size between 1 µm to 100 µm are assigned to the first range, the average grains sizes between 100 nm to 1000 nm to the second and the average grain sizes between 10 nm to 100 nm to the third. In the first range the volume fraction of intergranular phase shows a very small increase, which is less than 0.01, for the 2 orders of change in average grain sizes. In the second range the variation in volume fraction of intergranular phase is high when compared to the previous range but the variation is very much lower when compared to the final range. In the third range the variation in the volume fraction of intergranular phase is quite high given that the average grain size changes by one order. It shows clearly that the intergranular phase dominates when the average grain size less than 100 nm.

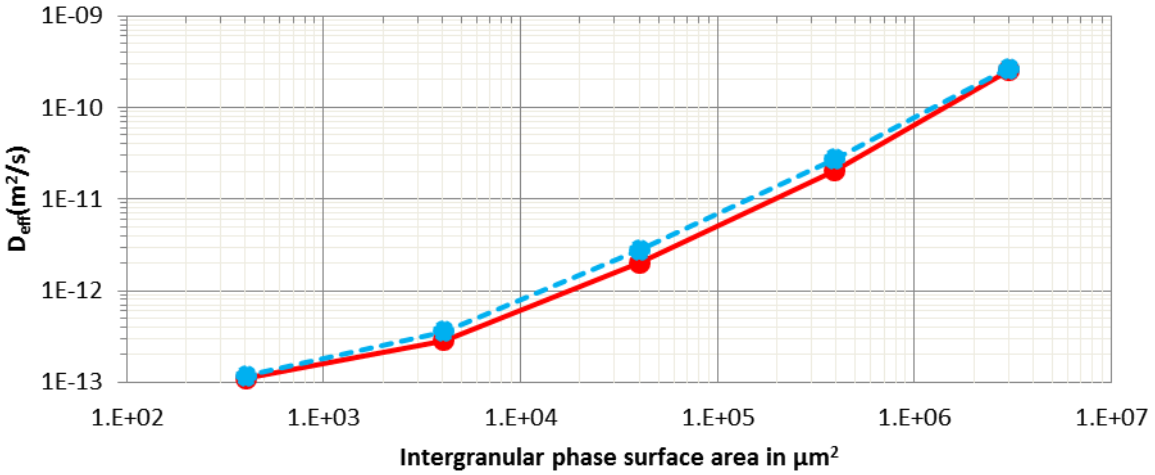

Figure 9: Computational results of effective mass diffusivity as the function of average surface area of intergranular phase (solid line) and analytical results (dotted line).

Figure 9 shows the evolution of effective mass diffusivity of heterogeneous polycrystalline composite media as the function of average surface area of intergranular phase, when the effective mass diffusivity of polycrystalline composite media decreases with the decrease in average surface area of intergranular phase. The decrease in intergranular surface area increases the average grain size of the polycrystalline material, in case of annealed

heterogeneous polycrystalline materials the decrease in grain size depend on the annealing properties such as temperature and time. The effective diffusivity of mass in heterogeneous polycrystalline composite media increases when the average surface area of intergranular phase increases.

5.2 Effective diffusivity of mass transport correlation with average grain size and intergranular phase:

Figure 10(a) shows the evolution of effective mass diffusivity of heterogeneous polycrystalline composite media as the function of average grain size. The effective diffusion of mass in heterogeneous polycrystalline composite media increases as the average grain size become smaller which increases the mobility of mass atom in the fine microstructure and the mobility of mass atom decreases in the coarse microstructure. The analytical results in dotted lines from Hashin-Shktrikman upper bound coincide with the Maxwell-Garnett effective medium approximation as expected and FE results calculated in solid lines are fitted good fit to these analytical results.

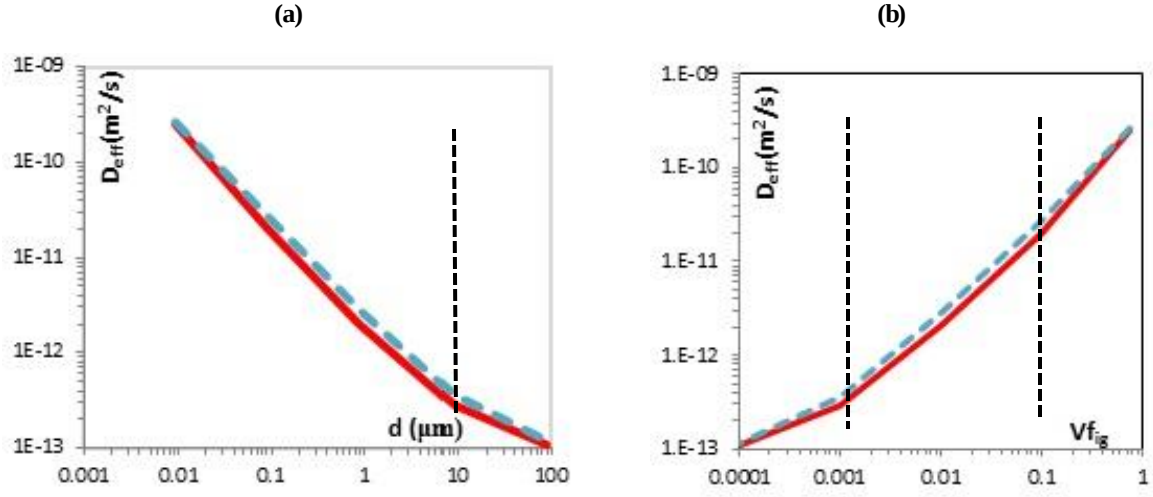

Figure 10: (a) Simulation results (solid line) and analytical (dotted line) for effective hydrogen diffusion coefficient as a function of average grain sizes (b) Simulation results (solid line) and analytical (dotted line) for effective hydrogen diffusivity as a function of volume fraction of intergranular phase.

Figure 10(b) shows the evolution of effective mass diffusivity of heterogeneous polycrystalline composite media as the function of volume fraction of intergranular microstructure phase. The effective diffusion of mass atom in heterogeneous polycrystalline composite media increases with the increase in the volume fraction of intergranular phase. The increase in surface area per unit volume of intragranular, increase in the average surface

of the intergranular phase and therefore the mobility of mass atom increases when the average grain sizes are in the fine microstructure. The decrease in intragranular surface area per unit volume decreases the average intergranular surface area which decreases the mobility of mass atom, when the average grain size is in the coarse microstructure. The analytical results in dotted line are good fitting with the calculated FE results.

5.3 Steady state normalized concentration of mass atom correlated with normalized distance for average grain size and intergranular phase:

The calculated results of the steady state normalized concentration of the GRVE, HRVE and MRVE are showed in Figure 11 as a function of normalized distance for five different average grain sizes. When the normalized distance of the GRVE increases, the normalized concentration decreases. The result curves are divided into two regions due to the difference in the hydrogen diffusivity between the HRVE and the MRVE. The left hand side region shows the normalized concentration profile of HRVE and the right hand side of the normalized concentration profile of MRVE for five different grain sizes. The variation of the normalized

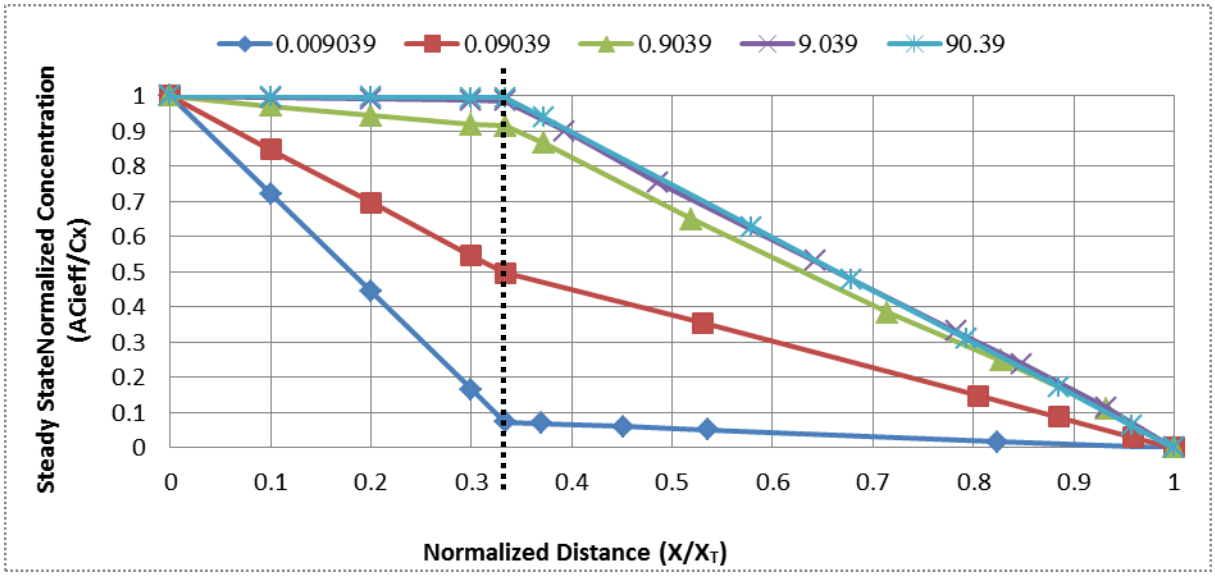

Figure 11: Computational results of normalized concentration of mass atom as the function of normalized distance of GRVE for various average grain sizes. The Curves are divided into two regions with the dotted line, the left side region shows the steady state normalized concentration profile of HRVE and the right side region shows the steady state normalized concentration profile of the MRVE. The diffusion coefficients assigned to HRVE is 1×10^{-11} m^2/s intergranular phase and intragranular phases are 9×10^{-14} m^2/s and 4×10^{-10} m^2/s respectively.

concentration with respect to normalized distance is higher in HRVE and smaller in MRVE for GRVE with nano grains, due to the higher area fraction of the intergranular phase. The variations of the normalized concentration with respect to the normalized distance are smaller in HRVE and higher in MRVE for GRVE for coarse grains, due to the smaller area fraction of the intergranular phase.

Figure 12 shows the normalized steady state concentration of hydrogen as the function of average grain sizes of the microstructure for seven different normalized distance of GRVE. The normalized steady state hydrogen concentration decreases with the decrease in the average grain size. The resultant curves are divided into two regions, in the first left side region in the Figure 12 for average grain size up to 1 µm, the increase in the normalized hydrogen concentration is higher with the increase in the grain size. In the second region i.e right side region in the Figure 12, the normalized steady state concentration of hydrogen attain saturated conditions and there is very little variation in normalized concentration of hydrogen for grain size higher than 1 µm up to 100 µm. For the top four normalized distance curves from 0.1 to 0.33 which belong to HRVE, there is no change in the normalized concentration for the grain sizes between 1 µm to 100 µm and then it decreases for the nano grain sizes less than 1000 nm and the difference in the normalized concentration between 1000 nm to 10 nm starts increasing when the normalized distance increases from 0.1 to 0.33. This difference in normalized concentration between 1000 nm to 10 nm starts decreasing when the normalized distance increases from 0.33 to 0.8, those distance belong to the MRVE.

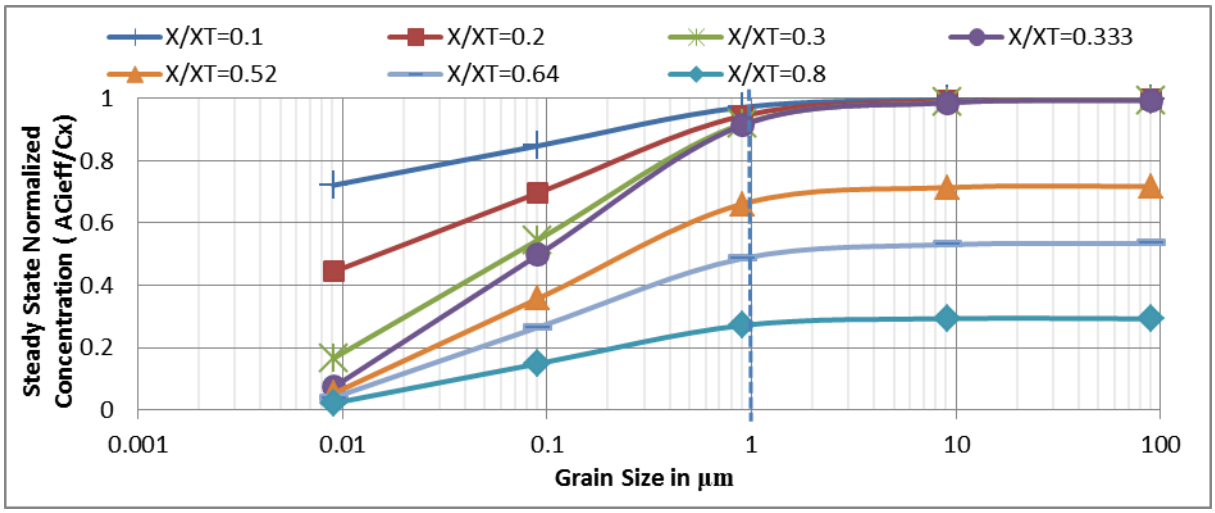

Figure 12: Calculated results of normalized steady state concentration of hydrogen atom as the function of average grain sizes for various normalized distance of GRVE.

6. Conclusion

The study of mass transport in heterogeneous polycrystalline intergranular and intragranular aggregates microstructural composite materials is important for establishing the relationship between microstructures and effective mass transport properties. A multiscale approach was adopted for the calculation. This paper has modelled the hydrogen diffusion behaviour of heterogeneous polycrystalline aggregate two phase composite media using the phase mixture based finite element model and investigated the influences of intergranular and intragranular microstructure and the effective hydrogen diffusivity. This modelling technique can also be applicable for multiphase as well multiscale (microstructure-micro scale, mesoscale, macrostructure-macro scale) heterogeneous polycrystalline composite structural media. The mass diffusion atom in heterogeneous polycrystalline intergranular and intragranular aggregates microstructural material with different grain sizes from micro to nanocrystalline by adjusting the volume fraction of the intergranular phase to the intragranular phase was modelled using both analytically and computationally which shows the good correlation between the results. The Figures 7, 8, 9 and 10 shows the numerical results performed good agreement with the analytical phenomena. The present study and investigation also illustrates that the mass diffusion in intergranular grain boundary becomes increasingly important as the grain size of the material decreases to nanocrystalline. This indicates the heterogeneous polycrystalline materials in the micro and nano scale range where the intergranular phase has an important role and cannot be ignored. These approaches allow the complex mass transport mechanism occurring in the intergranular microstructural phases to be modelled based on the grain sizes effects of the polycrystalline materials. The result obtained in this present study shows the higher the average surface area of intergranular phase, smaller the grain size of polycrystalline material. The polycrystalline composite materials grain boundary is incorporated with triple junctions within the current model. This treatment of the triple junctions is a limitation of this model.

Acknowledgements

This work was supported by EU 7^{th} framework program through the project MultiHy (Multiscale Modelling of Hydrogen Embrittlement) under project no. 263335.

References

1. G.Palumbo, D.M. Doyle, A.M.El-Sherik, U.Erb, K.T.Aust, Intercrystalline hydrogen diffusion transport in nanocrystalline nickel, Scripta Metall. 25 (1991) 679-684.
2. T.M.Harris, R.M.Latanision, Grain boundary diffusion of hydrogen in nickel, Metallurgical Transactions A, 22A (1991) 351-355.
3. A.Oudriss, J .Creus, J.Bouhattate, E.Conforto, C.Berziou, C.Savall, X.Feaugas, Grain size and grain boundary effects on diffusion and trapping of hydrogen in pure nickel, Acta Materialia 60 (2012) 6814-6828.
4. T.Tsuru, R.M.Latanision, Grain boundary transport of hydrogen in nickel, Scripta Metall 16 (1982) 575-578.
5. B.S.Bokstein, H.D.Brose, L.I.Trusov, T.P.Khvostantseva, Diffusion in nanocrystalline nickel, NanoStructured Materials 6 (1995) 873-876.
6. A.Portavoce, G.Chai, L.Chow, J.Bernardini, Nanometric size effect on Ge diffusion in polycrystalline Si, J Appl Phys 104 (2008) 104910:1-8.
7. Shun Li, Jianqiu Zhou, Lu Ma, Nan Xu, Rongtao Zhu, Xiaohua He, Continuum level simulation on the deformation behaviour of nanocrystalline nickel, Computational Mater Sci 45 (2009) 390-397.
8. T.Watanabe, Grain boundary engineering: historical perspective and future prospects, J Mater Sci 46 (2011) 4095-4115.
9. C.A.Schuh, M.Kumar, W.E.King, Universal features of grain boundary networks in FCC materials, J Mater Sci 40 (2005) 847-852.
10. C.A.Schuh, R.W.Minich, M.Kumar, Connectivity and percolation in simulated grain boundary networks, Philosophical Magazine 83 (2003) 711-726.
11. R.M.Latanision, H.Opperhauser Jr., The intergranular embrittlement of nickel by hydrogen: the effect of grain boundary segregation, Metrall Trans 5 (1974) 483-492.
12. S.Kobayashi, S.Tsurekawa, T.Watanabe, G.Palumbo, Grain boundary engineering for control of sulfur segregation induced embrittlement in ultrafine-grained nickel, Scripta Mater 62 (2010) 294-297.
13. S.Ghosh, S.Moorthy, Three dimensional Voronoi cell finite element model for microstructures with ellipsoidal heterogeneities, Computational Mechanics 34 (2004) 510-531.
14. J.C.Fisher, Calculation of diffusion penetration curves for surface and grain boundary diffusion, J Appl Phy 22 (1951) 74-77.
15. R.E.Hoffman, D.Turnbull, Lattice and grain boundary self-diffusion in silver, J Appl Phys 22 (1951) 634-639.

16. D.Turnbull, R.E.Hoffman, The effect of relative crystal and boundary orientations on gran boundary diffusion rates, Acta Metallurgica 2 (1954) 419-426.
17. E.W.Hart, On the role of dislocations in bulk diffusion, Acta Metallurgica 5 (1957) 597.
18. H.Wang, W.Yang, A.H.W.Ngan, Enhanced diffusivity by triple junction networks, Scripta Materialia 52 (2005) 69-73.
19. I.V.Belova, G.E.Murch, Diffusion in nanocrystalline materials, J Phys Chem Solids 66 (2003) 873-878.
20. I.M.Bernstein, The role of Hydrogen: is the story any clearer?, Hydrogen effects in Materials, eds. A.W.Thompson and N.R.Moody (1996) 3-11.
21. A.R.Troiano, The role of Hydrogen and Other Interstitials on the Mechanical Behavior of Metals, Trans. American Society for Metals 52 (1960) 54.
22. A.Turnbull, Modelling of environment assisted cracking, Corrosion Science 34 (1993) 921-960.
23. A.Turnbull, M.W.Carroll, D.H.Ferriss, Analysis of hydrogen diffusion and trapping in a 13 % chromium martensitic stainless steel, Acta Metall. 37 (1989) 2039-2046.
24. J.P.Hirth, The influence of grain boundaries on mechanical properties, Metallurgical Transactions 3 (1972) 3047-3067.
25. A.H.M.Korm, Numerical modelling of hydrogen transport in steel, PhD Thesis (1998).
26. R.M.Latanision, H.Opperhauser.Jr, Further observations on the effect of grain boundary segregation in the hydrogen embrittlement of nickel, Metallurgical Transactions A 6A (1975) 233-234.
27. G.Palumbo, F.Gonzalez, A.M.Brennenstuhl, U.Erb, W.Shmayda, P.C.Lichtenberger, In-situ nuclear steam generator repair using electrodeposited nanocrystalline nickel, Nanostructured Materials 9 (1997) 737-746.
28. M.L.Martin, B.P.Somerday, R.O.Ritchie, P.Sofronis, I.M.Robertson, Hydrogen-induced intergranular failure in nickel revisited, Acta Materialia 60 (2012) 2739-2745.
29. A.J.Mortlock, The effect of segregation on the solution diffusion enhancement due to the presence of dislocations, Acta Metallurgica 8 (1960)132-134.
30. J.R.Kalnin, E.A.Kotomin, V.N.Kuzovkov, Calculation of the effective diffusion coefficient in inhomogeneous solids, Defect and Diffusion Forum 163 (2001) 194-199.
31. J.C.Maxwell Garnett, Colours in metal glasses and in metallic films, Phil. Trans. R. Soc. London A 203 (1904) 385-420.
32. M.A.Meyers, A.Mishra, D.J.Benson, Mechanical properties of nanocrystalline materials, Progress in Materials Science 51 (2006) 427-556.

33. E.Lauridson, S.Schmit, S.Nielsen, L.Margulies, H.Poulsen, D.Jensen, Non-destructive characterization of recrystallization kinetics using three-dimensional X-ray diffraction microscopy, Scripta Mater 55 (2006) 51-56.
34. B.Adams, T.Olson, The mesostructure-properties linkage in polycrystals, Progress Mater Sci 43 (1998) 1-88.
35. F.Fritzen,T.Bohlke,E.Schnack, Periodic three-dimensional mesh generation for crystalline aggregates based on Voronoi tessellations, Comput Mech 43 (2009) 701-713.
36. M.Groeber, B.Haley, M.Uchic, D.Dimiduk, S.Ghosh, 3D reconstruction and characterization of polycrystalline microstructure using a FIB-SEM, Mater Characterization 57 (2006) 259-273.
37. Y.Bhandari, S.Sarkar, M.Groeber, M.Uchic, D.Dimiduk, S.Ghosh, 3D polycrystalline microstructure reconstruction from FIB generated serial sections for FE analysis, Comput Mater Sci 41 (2007) 222-235.
38. James Clerk Maxwell, A Treatise on electricity and Magnetism, Oxford: Clarendon Press I, II (1873).
39. M.Felberbaum, E.Landry-Desy, L.Weber, M.Rappaz, Effective hydrogen diffusion coefficient for solidifying aluminium alloys, Acta Materialia 59 (2011) 2302-2308.
40. Z.Hashin, S.Shtrikman, A variational approach to the theory of the effective magnetic permeability of multiphase materials, J Appl Phys 33 (1962) 3125-3131.
41. Y.Chen, C.A.Schuh, Geometric consideration for diffusion in polycrystalline solids, J Appl Phys 101 (2007) 063524:1-12.
42. H. Gleiter, Nanocrystalline materials, Progress in Materials Science 33 (1989) 223-315.